Buckling Analysis of Discontinues Fractional Axially Graded Thin Beam with Piecewise Axial Load Function Rested on Rotational Spring Hinges

Abbas Heydari *

Department of civil engineering, Faculty of Razi, Ardabil branch,
Technical and Vocational University (TVU), Ardabil, Iran
E-mail: a_heydari@tabrizu.ac.ir
*Corresponding author

Abstract: Functionally Graded Materials (FGMs) can be described by continuous variation in structure and composition over volume, resulting in corresponding changes in the properties of the material. These kinds of materials are designed to achieve specific properties for specific applications. For the first time, the effects of stepwise fractional axial material gradation pattern and axial compressive load with piecewise function on buckling behaviour of Euler-Bernoulli beam rested on semi-rigid restraints are studied. It is worth mentioning that the more computational efforts are required to solve current problem with respect to the buckling problem of transversely graded beam due to discontinues material gradation especially in the axial direction, axial span-load with piecewise function and natural conditions of rotational spring hinges. The deflection continuity, natural equations as well as boundary conditions are written in the matrix form. The beam discretizing and nontrivial solution are employed to obtain buckling characteristic equation and matrix operations are used to calculate corresponding first mode shapes. Compatibility with various conditions and eliminating convergence drawbacks of conventional numerical tools are advantages of the proposed method. It is observed that the buckling load is decreased by increasing lengths of beam parts and increased by increasing rotational stiffness at semi-rigid supports. In the case of homogeneous beam, the result validity is proved by observing an excellent agreement between results of current work and well-known data in literature.

Reference: Abbas Heydari, "Buckling Analysis of Discontinues Fractional Axially Graded Thin Beam with Piecewise Axial Load Function Rested on Rotational Spring Hinges", Int J of Advanced Design and Manufacturing Technology, Vol. 13/No. 2, 2020, pp. 99–108.

Biographical notes: Abbas Heydari received his PhD in Civil Engineering major of Structural Engineering from University of Tabriz in 2017. He is currently Technical Assistant Professor at the Department of civil Engineering, Technical and Vocational University (TVU), Ardabil, Iran. His current research interest includes study on mechanical behaviour of structural members made up of bidirectional functionally graded materials, stability and vibration of structures, size-dependent analysis, Elasto-Plastic analysis of reservoirs and shear deformation theories. Moreover, his researches are focused on numerical tools to solve governing equations arisen from various engineering problems.

1   INTRODUCTION

The sharp transition of properties at the junction of conventional composite materials is eliminated by inventing a novel type of composite materials named Functionally Graded Materials (FGMs). This material was first invented in 1984 by Japanese scientists for the core purpose of their aerospace project that required thermal barrier with the outside temperature of 2000 k and inside temperature of 1000 k within 1cm thickness. FGMs are described by continuous variation in structure and composition over volume, resulting in corresponding changes in the properties of the material. They are designed to achieve specific properties for specific applications.

The various benefits of FGMs over conventional composites attract many researchers to analyze structures made up of FGMs. In addition, various complexities in current work like the fractional material gradation in axial direction, discontinues axial load and mechanical properties as well as semi-rigid supports at beam ends required a robust solution method.

The thermal snap-buckling analysis of temperature-dependent functionally graded curved Nano beam with clamped ends subjected to uniform temperature distributions across the thickness is conducted. The size effects are captured by nonlocal strain gradient theory. Hamilton's principle and Akavci's beam theory are used to derive nonlinear governing equations. The effects of strain gradient parameter, nonlocal parameter, thermal loadings and power law index on the snap-buckling of the Nano beam are investigated [1].

The wave propagation in double-layered porous nanotubes systems is investigated by considering nonlocal strain gradient theory and using the Hamilton principle. It is observed that the material properties of nanotubes are depended on the porosity and hygro-thermal effects. The dispersion relations and displacement fields of wave propagation in the double nanotubes systems which experience three different types of motion are obtained and discussed. The phase velocities of the double nanotubes systems are affected by various parameters including non-local and strain gradient parameters, temperature and humidity change, porosity, material composition, interlayer spring and wave number [2].

The snap-buckling analysis of nonlocal Reddy's higher-order functionally graded porous curved beam resting on three parameters elastic medium subjected to uniform transverse load with immovable simply-supported or clamped boundary conditions is performed. By using the two-step perturbation technique, the perturbation equations and the approximate boundary value problems of nonlinear governing equations are obtained. The effects of small scale, elastic foundation, porosity, material composition, geometry and boundary conditions are studied [3]. According to the nonlocal strain gradient theory assumptions, the nonlinear bending analysis of porous functionally graded curved nanotubes with uniformly distributed pores in the radial direction by considering the stiffness reduction and enhancement effects is done.

The asymptotic solutions of the curved nanotubes are obtained via two-step perturbation method. The jump changes as well as snap-through buckling can occur when the functionally graded curved nanotubes are affected by normal bending loads [4]. The prediction of wave propagation behaviors of functionally graded materials porous Nano beams based on Reddy's higher-order shear deformation beam theory in conjunction with the nonlocal strain gradient theory is presented. By employing Hamilton principle, governing equations of the porous nan beams are derived. The analytic dispersion relation is obtained by solving an eigenvalue problem.

The results of thin beam based on classical or Euler-Bernoulli beam theory and results of Timoshenko beam based on first order shear deformation beam model are calculated [5]. Within the framework of the nonlocal strain gradient theory, the nonlinear bending and vibrational characteristics of size-dependent shear deformable radially graded porous tube are analyzed. The feasibility and validity of the applied method are verified by actual examples. The effects of different parameters such as porosity volume fraction, power law index, scaling parameters and inner-to-outer radius ratio on the nonlinear bending and vibration behaviors of the porous tubes are discussed [6]. An analytic model of porous nanotubes for the wave propagation analysis is formulated with the help of the nonlocal strain gradient theory.

The dispersion relations between phase velocity and wave number are determined by solving an eigenvalue problem. It is found that the asymptotic phase velocity can be increased by increasing the strain gradient parameter or decreasing the nonlocal parameter. Moreover, the heterogeneity of functionally graded materials and temperature variation has a substantial influence on the dispersion relations of nanotubes. The nonlocal parameter and strain gradient parameter have important effects on the dispersion relation at high wave numbers; in contrast, these effects can be negligible at low wave numbers. Meanwhile, it can be inferred that the phase velocity can decrease or increase as the porosity volume fraction rises, which depends on the power law index [7]. The vibration problem of size-dependent and temperature-dependent refined porous nanotubes is solved via Navier method [8]. The buckling and postbuckling behaviors of nanotubes are studies thoroughly [9]. Thermal buckling and post-buckling analysis of functionally graded beams based on a general higher-order shear deformation theory is conducted [10].

The numerical tools like the ANFIS [11] and DTM [12] are the essential tools to solve engineering problems [13-14].

The calculus of variations and collocation method are employed to solve buckling problem of tapered Euler-Bernoulli Nano-beams made up of bidirectional functionally graded material under variable axial compression in the presence of elastic medium [15]. The spectral Ritz method with trial functions of orthogonal shifted Legendre polynomials is used to solve buckling problem of thick functionally graded circular plate rested on Pasternak foundation [16]. The modified Chebyshev-Ritz method without adhesive or auxiliary functions requirement is employed to analyze size-dependent damped vibration and buckling analyses of bidirectional functionally graded solid circular Nano-plate with arbitrary thickness variation [17]. A new methodology based on differential transform and collocation methods is proposed to solve coupled partial differential equations of motion without any simplifications [18].

A new scheme for buckling analysis of bidirectional functionally graded Euler beam having arbitrary thickness variation rested on Hetenyi elastic foundation is proposed [19]. The analytical method is used to conduct various analyses including buckling analysis of functionally graded tube, beam and plate [20-23]. The effect of attached lumped mass position on the frequency reduction of the radially graded tube is investigated by employing spectral Ritz method [24]. Elastic buckling analysis of multistory functionally graded sway bending frame is performed via finite element method [25]. Elastic buckling analysis of non-sway bending frame is performed by using stability functions [26].

This work aims to investigate the effects of fractional material gradation in the axial direction as well as piecewise axial compressive load function on buckling behavior of Euler-Bernoulli beam. The problem requires a robust methodology due to complicated conditions including stepwise material gradation in the axial direction, axial span-load and natural conditions at rotational spring hinges. Current work presents an efficient and simple method to conduct buckling analysis of discontinues fractional axially graded thin beam with piecewise axial load function rested on semi-rigid restraints.

The nontrivial solution is used to calculate buckling characteristic equation of beam and matrix operations are used to obtain corresponding buckling mode shapes of first buckling loads. Compatibility with various conditions and eliminating convergence drawbacks of conventional numerical tools are advantages of the proposed method. The validity of the proposed method is proved by observing an excellent agreement between results of present work for homogeneous beam with the well-known data in literature.

2 GOVERNING EQUATIONS

The stepwise fractional axially graded Euler-Bernoulli beam subjected to axial span-load rested on semi-rigid restraint is illustrated in "Fig. 1". The beam is made of two distinct parts with different lengths but same axial material gradation. The right part of the beam with the length $L_2 = L_r$, is subjected to the concentrated axial load, P, but the left part of the beam with the length $L_1 = L_l$ is axial-stress-free. The rotational stiffness of rotational spring hinges at left and right ends of the beam are $k_{\theta l}$ and $k_{\theta r}$, respectively.
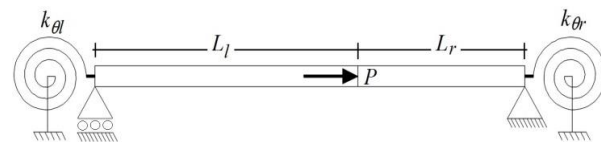
Fig. 1 Stepwise fractional axially graded beam with semi-rigid support subjected to axial span-load.

In fractional material gradation model, the gradation power function is to the power of a fraction rather than a whole number. In current work, the elasticity modulus gradation of fractional axially graded Euler-Bernoulli beam is modeled by one and a half fraction power function.

$$E_i(x) = E_0 \left(1 + \frac{x_i}{L_i}\right)^{1.5} \qquad i \in \{1,2\} \qquad (1)$$

The parameter L_i is beam length, which takes $L_1 = L_l$ or $L_2 = L_r$. The parameter E_0 is material index. The elasticity modulus value at left end of the beam parts is E_0. The elasticity modulus at right end of the beam parts is $2\sqrt{2}E_0$. The total potential energy can be written as follows:

$$\Pi = U + \Omega \qquad (2)$$

The stored strain energy and path-dependent work caused by non-conservative force are shown by U and Ω, respectively. The total potential energy of buckled fractional axially graded Euler-Bernoulli beam element is:

$$\Pi = \frac{1}{2} I \int_0^L E(x) \left(\frac{d^2}{dx^2} w(x)\right)^2 dx - \frac{1}{2} P \int_0^L \delta l(x) \qquad (3)$$

Where, the parameters I, w, P and $\delta l(x)$ denote moment of inertia, deflection, concentrated axial compression applied to the beam end and change of the beam element

length caused by buckling at the position x, respectively. It is noteworthy that the parameter $\delta l(x)$ takes positive sign when decrease in length occurs. The total change of the beam length subjected to compressive load is calculated as follows:

$$\Delta L = \int_0^L \left(\sqrt{1 + (dw(x)/dx)^2} - 1 \right) dx \qquad (4)$$

The integrand in second term of "Eq. (3)" is replaced by truncated Taylor series expansion with truncation order of three. "Eq. (3)" is rewritten as follows:

$$\Pi = \frac{1}{2} I \int_0^L E(x) \left(\frac{d^2}{dx^2} w(x) \right)^2 dx - \frac{1}{2} P \int_0^L \left(\frac{d}{dx} w(x) \right)^2 dx \qquad (5)$$

The total potential energy must be minimized to calculate governing equilibrium equation. To this purpose, instead of w, the auxiliary path, $\widetilde{w}$, is assumed.

$$\widetilde{w}(x) = w(x) + \lambda \varphi(x) \qquad (6)$$

The smooth function $\varphi(x)$ can be differentiated twice. Moreover, $\varphi(x)$ and its derivatives are vanished at both ends of the beam element. The derivative of Π with respect to λ is calculated to minimize total potential energy. The numeral constant λ is approached to zero to match the auxiliary path to the initial path.

$$\lim_{\lambda \to 0} \frac{\partial}{\partial \lambda} \left(I \int_0^L E(x) \left(\frac{d^2}{dx^2} \widetilde{w} \right)^2 dx - P \int_0^L \left(\frac{d}{dx} \widetilde{w} \right)^2 dx \right) = 0 \qquad (7)$$

The chain rule is employed as follows:

$$\frac{1}{2} \lim_{\lambda \to 0} I \int_0^L \left(E(x) \frac{\partial}{\partial \widetilde{w}''} (\widetilde{w}'')^2 \frac{\partial \widetilde{w}''}{\partial \lambda} dx - P \int_0^L \frac{\partial}{\partial \widetilde{w}'} (\widetilde{w}')^2 \frac{\partial \widetilde{w}'}{\partial \lambda} dx \right) = 0 \qquad (8)$$

"Eq. (8)" is simplified as follows:

$$I \int_0^L E \frac{d^2}{dx^2} w(x) \frac{d^2}{dx^2} \varphi(x) dx - P \int_0^L \frac{d}{dx} w(x) \frac{d}{dx} \varphi(x) \, dx = 0 \qquad (9)$$

According to integration by parts rule, one can write:

$$I \int_0^L E(x) \frac{d^2}{dx^2} w(x) \frac{d^2}{dx^2} \varphi(x) dx - P \int_0^L \frac{d}{dx} w(x) \frac{d}{dx} \varphi(x) dx =$$

$$E(x) I \left(\frac{d^2}{dx^2} w(x) \frac{d}{dx} \varphi(x) \right) - P \left(\frac{d}{dx} w(x) \varphi(x) \right) \Bigg]_{x=0}^{x=L} \qquad (10)$$

$$-I \int_0^L \frac{d}{dx} \varphi(x) \frac{d}{dx} \left(E(x) \frac{d^2}{dx^2} w(x) \right) dx$$

$$+P \int_0^L \frac{d^2}{dx^2} w(x) \varphi(x) dx = 0$$

The integration by parts rule can be employed again.

$$-I \int_0^L \frac{d}{dx} \varphi(x) \frac{d}{dx} \left(E(x) \frac{d^2}{dx^2} w(x) \right) dx$$

$$+P \int_0^L \frac{d^2}{dx^2} w(x) \varphi(x) dx =$$

$$-I \frac{d}{dx} \left(E(x) \frac{d^2}{dx^2} w(x) \right) \varphi(x) \Bigg]_{x=0}^{x=L} + \qquad (11)$$

$$\int_0^L \left(I \frac{d^2}{dx^2} \left(E(x) \frac{d^2}{dx^2} w(x) \right) + P \varphi(x) \frac{d^2}{dx^2} w(x) \right) dx = 0$$

"Eq. (11)", implies that the integrand must be set equal to zero. The equilibrium equation is obtained as follows:

$$E_0 I \big((L + x)^2 w^{(4)} + 3(L + x) w^{(3)} + (3/4) w^{(2)} \big) \qquad (12)$$

$$+ P L^2 \sqrt{1 + (x/L)} \, w^{(2)} = 0$$

3   DEFLECTION FUNCTION

According to "Fig. 2", the local coordinates are assigned to each part of the beam to calculate deflection functions.
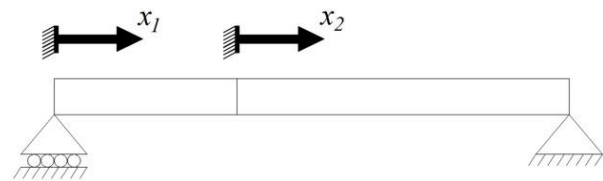
Fig. 2   Local coordinates for beam parts.

The solution of the governing differential equation is:

$$w(x_2) = c_1 w_1(x_2) + c_2 w_2(x_2) + w_{rbm}(x_2) \qquad (13)$$

The function $w_{rbm}(x_2)$ denotes rigid body motion of the right part of the beam element.

$$w_{rbm}(x_2) = c_3 x_2 + c_4 \quad (14)$$

The bases $w_1(x_2)$ and $w_2(x_2)$ are:

$$\begin{aligned} & w_1(x_2) \\ &= J_2\left(4\sqrt[4]{L_2+x_2}\sqrt{PL_2^{3/2}/E_0 I}\right)\sqrt{L_2+x_2} \end{aligned} \quad (15)$$

$$\begin{aligned} & w_2(x_2) \\ &= Y_2\left(4\sqrt[4]{L_2+x_2}\sqrt{PL_2^{3/2}/E_0 I}\right)\sqrt{L_2+x_2} \end{aligned} \quad (16)$$

Where, J and Y are Bessel functions of the first and second kinds, which are one of a class of special functions related to the hypergeometric functions that arise as solutions of Bessel's equation. Standard solutions are known as the Bessel functions of the first and second kinds, J and Y, respectively. The subscript two denotes the order of the Bessel functions. By approaching P to zero, the deflection of fractional axially graded beam in the absence of axial compression will be obtained.

$$\bar{w}(x_1) = c_5 \bar{w}_1(x_1) + c_6 \bar{w}_2(x_1) + \bar{w}_{rbm}(x_1) \quad (17)$$

The function $\bar{w}_{rbm}(x_1)$ denotes rigid body motion of the beam element.

$$\bar{w}_{rbm}(x_1) = c_7 x_1 + c_8 \quad (18)$$

The bases $\bar{w}_1(x_1)$ and $\bar{w}_2(x_1)$ are:

$$\bar{w}_1(x_1) = \sqrt{L_1+x_1} \quad (19)$$

$$\bar{w}_2(x_1) = \sqrt{(L_1+x_1)^3} \quad (20)$$

4   CHARACTERISTIC EQUATION

The problem includes eight homogeneous equations. A system of linear equations is homogeneous if all of the constant terms are zero. The solutions involving the number zero are considered trivial, while nonzero solutions are considered nontrivial. The required equations for calculating characteristic equation of beam are:

$$\bar{w}|_{x_1=0} = 0 \quad (21)$$

$$\left(E_1 I \frac{d^2}{dx_1^2}\bar{w}\right)\bigg|_{x_1=0} - k_{\theta l}\left(\frac{d}{dx_1}\bar{w}\right)\bigg|_{x_1=0} = 0 \quad (22)$$

$$w|_{x_2=L_r} = 0 \quad (23)$$

$$\left(E_2 I \frac{d^2}{dx_2^2}w\right)\bigg|_{x_2=L_r} + k_{\theta r}\left(\frac{d}{dx_1}w\right)\bigg|_{x_2=L_r} = 0 \quad (24)$$

$$\bar{w}|_{x_1=L_l} - w|_{x_2=0} = 0 \quad (25)$$

$$\left(\frac{d}{dx_1}\bar{w}\right)\bigg|_{x_1=L_l} - \left(\frac{d}{dx_2}w\right)\bigg|_{x_2=0} = 0 \quad (26)$$

$$2\sqrt{2}E_0 I\left(\frac{d^2}{dx_1^2}\bar{w}\right)\bigg|_{x_1=L_l} - E_0 I\left(\frac{d^2}{dx_2^2}w\right)\bigg|_{x_2=0} \\ = 0 \quad (27)$$

$$\frac{d}{dx_1}\left(E_1 I \frac{d^2}{dx_1^2}\bar{w}\right)\bigg|_{x_1=L_l} \\ - \frac{d}{dx_2}\left(E_2 I \frac{d^2}{dx_2^2}w\right)\bigg|_{x_2=0} \\ = 0 \quad (28)$$

"Eq. (21) to Eq. (28)" are written in the matrix form.

$$\begin{bmatrix} m_{11}(P) & \cdots & m_{18}(P) \\ \vdots & \ddots & \vdots \\ m_{81}(P) & \cdots & m_{88}(P) \end{bmatrix}_{8\times8} \begin{Bmatrix} c_1 \\ \vdots \\ c_8 \end{Bmatrix}_{8\times1} = \begin{Bmatrix} 0 \\ \vdots \\ 0 \end{Bmatrix}_{8\times1} \quad (29)$$

In the next step, the rows that include only one nonzero array and corresponding columns are deleted. The characteristic equation is calculated by vanishing determinant of the reduced coefficient matrix.

$$\begin{vmatrix} m_{11}(P) & \cdots & m_{1(8-r)}(P) \\ \vdots & \ddots & \vdots \\ m_{(8-r)1}(P) & \cdots & m_{(8-r)(8-r)}(P) \end{vmatrix}_{(8-r)\times(8-r)} \\ = 0 \quad (30)$$

The parameter r denotes number of removed rows or columns. The γth mode shape of buckled beam can be calculated as follows:

$$\begin{Bmatrix} c_1 \\ \vdots \\ c_{7-r} \end{Bmatrix}_{(7-r)\times1} = -c_{(8-r)}$$

$$\begin{bmatrix} m_{11}(P_\gamma) & \cdots & m_{1(7-r)}(P_\gamma) \\ \vdots & \ddots & \vdots \\ m_{(7-r)1}(P_\gamma) & \cdots & m_{(7-r)(7-r)}(P_\gamma) \end{bmatrix}^{-1}_{(7-r)\times(7-r)} \quad (31)$$

$$\begin{Bmatrix} m_{1(8-r)}(P_\gamma) \\ \vdots \\ m_{(7-r)(8-r)}(P_\gamma) \end{Bmatrix}_{(7-r)\times1}$$

in which P_γ is the γth positive root of the characteristic equation ($P_\gamma \in \mathbb{R}$).

5   RESULT VALIDATION

The dimensionless buckling loads of first three modes of prismatic homogeneous beam with various classical boundary conditions are available in literature. The proposed method in current work is used to calculate first three dimensionless buckling loads of Euler-Bernoulli beam with pinned-clamped boundary conditions to prove validity of the calculated results based on proposed method by observing an excellent agreement between current work results and results of available data in literature. The intact beam is discretized to two distinct parts with the same mechanical properties and section dimensions, but different lengths L_1 and L_2. It is assumed that the axial compression load is applied at the end of the beam; consequently, the deflection functions of the beam parts can be calculated as follows:

$$y_i(x_i) = c_{1+j} + c_{2+j}x_i + c_{3+j}\sin(Fx_i) + c_{4+j}\cos(Fx_i) \tag{32}$$

In which, $i \in \{1,2\}$ and j takes 0 or 4 for $i = 1$ or $i = 2$, respectively. Also, the parameter F is $\sqrt{P/EI}$. Boundary conditions for simply supported-clamped beam are:

$$y_1|_{x_1=0} = 0 \tag{33}$$

$$y_2|_{x_2=L_2} = 0 \tag{34}$$

$$\frac{d^2}{dx_1^2}y_1\bigg|_{x_1=0} = 0 \tag{35}$$

$$\frac{d}{dx_2}y_2|_{x_2=L_2} = 0 \tag{36}$$

The continuity of deflection at junction of two parts implies that "Eq. (37) and Eq. (38)" must be satisfied.

$$y_1|_{x_1=L_1} - y_2|_{x_2=0} = 0 \tag{37}$$

$$\frac{d}{dx_1}y_1\bigg|_{x_1=L_1} - \frac{d}{dx_2}y_2\bigg|_{x_2=0} = 0 \tag{38}$$

The equilibrium of bending moment and shear force at junction of two parts are explained by "Eq. (39) and Eq. (40)".

$$\frac{d^2}{dx_1^2}y_1\bigg|_{x_1=L_1} - \frac{d^2}{dx_2^2}y_2\bigg|_{x_2=0} = 0 \tag{39}$$

$$\frac{d^3}{dx_1^3}y_1\bigg|_{x_1=L_1} - \frac{d^3}{dx_2^3}y_2\bigg|_{x_2=0} = 0 \tag{40}$$

"Eq. (33) to Eq. (40)" are written in the matrix form. The coefficient matrix, m_{ij} ($i,j \in \{1,2,3,...,8\}$), is presented in "Eq. (41)". In the next step, the rows that include only one nonzero array and corresponding columns are deleted. Because of zero arrays, the 3rd row and corresponding column (4th column) of coefficient matrix in "Eq. (41)" are eliminated. The similar elimination is used for 1st row and 1st column of the remained matrix in "Eq. (42)" to obtain the reduced coefficient matrix ($C_v = \cos(FL_v), S_v = \sin(FL_v)$).

$$\begin{bmatrix} 1 & 0 & 0 & 1 & 0 & 0 & 0 & 0 \\ 0 & 0 & 0 & 0 & 1 & L_2 & S_2 & C_2 \\ 0 & 0 & 0 & -F^2 & 0 & 0 & 0 & 0 \\ 0 & 0 & 0 & 0 & 0 & 1 & FC_2 & -FS_2 \\ 1 & L_1 & S_1 & C_1 & -1 & 0 & 0 & -1 \\ 0 & 1 & FC_1 & -FS_1 & 0 & -1 & -F & 0 \\ 0 & 0 & -F^2S_1 & -F^2C_1 & 0 & 0 & 0 & F^2 \\ 0 & 0 & -F^3C_1 & F_3S_1 & 0 & 0 & F^3 & 0 \end{bmatrix} \tag{41}$$

$$\begin{bmatrix} 0 & 0 & 0 & 1 & L_2 & S_2 & C_2 \\ 0 & 0 & 0 & 0 & 1 & FC_2 & -FS_2 \\ 1 & L_1 & S_1 & -1 & 0 & 0 & -1 \\ 0 & 1 & FC_1 & 0 & -1 & -F & 0 \\ 0 & 0 & -F^2S_1 & 0 & 0 & 0 & F^2 \\ 0 & 0 & -F^3C_1 & 0 & 0 & F^3 & 0 \end{bmatrix} \tag{42}$$

$$\begin{bmatrix} 0 & 0 & 1 & L_2 & S_2 & C_2 \\ 0 & 0 & 0 & 1 & FC_2 & -FS_2 \\ L_1 & C_1 & -1 & 0 & 0 & -1 \\ 1 & FC_1 & 0 & -1 & -F & 0 \\ 0 & -F^2S_1 & 0 & 0 & 0 & F^2 \\ 0 & -F^3C_1 & 0 & 0 & F^3 & 0 \end{bmatrix} \tag{43}$$

The buckling characteristic equation will be obtained by calculating determinant of reduced coefficient matrix in "Eq. (43)". It is worth mentioning that the roots of characteristic equation calculated from coefficient matrix in "Eq. (41)" and roots of characteristic equation calculated from reduced coefficient matrix in "Eq. (43)" are similar, but using reduced coefficient matrix results into decreasing of computational efforts to calculate corresponding mode shapes. The characteristic equation of homogeneous beam with pinned-clamped boundary conditions is calculated as follows:

$$\begin{aligned}(\cos(FL_1)\cos(FL_2) \\ - \sin(FL_1)\sin(FL_2))F(L_1 \\ + L_2) \\ -(\cos(FL_1)\sin(FL_2) + \sin(FL_1)\cos(FL_2)) \\ = 0\end{aligned} \tag{44}$$

The characteristic equation can be simplified by considering this fact that the total length of the beam is $L = L_1 + L_2$.

$$\tan(FL) = FL \qquad (45)$$

The first three positive real roots of "Eq. (46)" are 4.4934, 7.7253 and 10.9041. The first three dimensionless buckling loads ($\pi^2 EI/L^2$) are calculated as 2.0457, 6.0468 and 12.0471. These results are available in literature; therefore, the validity of the proposed method is proved. The coefficients c_1 and c_4 are set equal to zero. The modified bases of two separate parts are recalculated and the unknown coefficients' subscripts are resorted ($\bar{x}_2 = x_2 - L_1$).

(a) : First mode shape

(b) : Second mode shape

(c) : Third mode shape
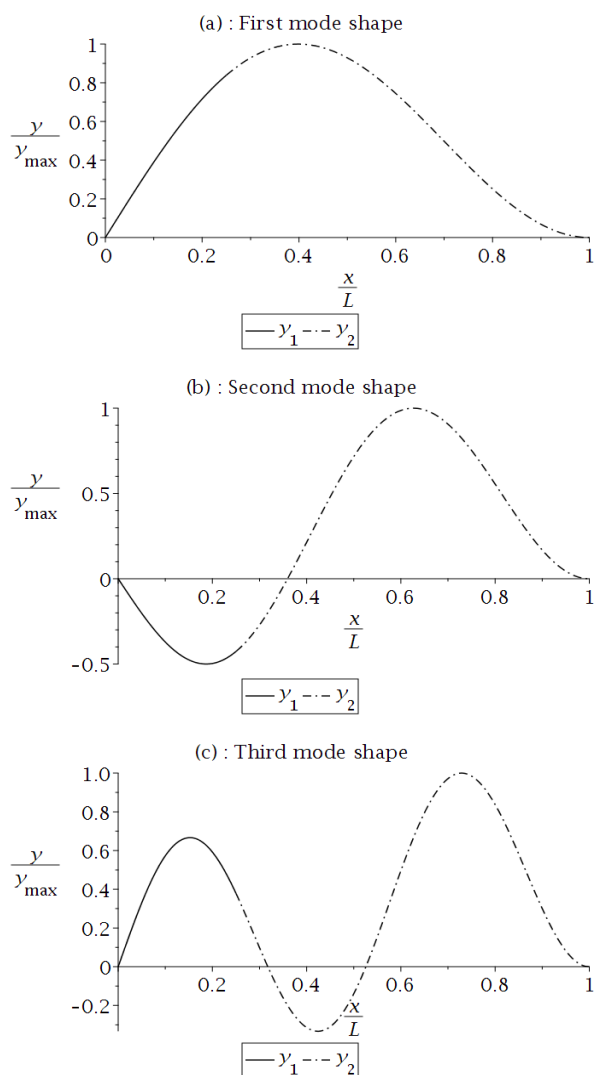
Fig. 3   Normalized first three mode shapes of homogeneous beam.

$$y_1(x_1) = c_1 x_1 + c_2 \sin(Fx_1) \qquad (46)$$

$$y_2(\bar{x}_2) = c_3 + c_4 \bar{x}_2 + c_5 \sin(F\bar{x}_2) \\ + c_6 \cos(F\bar{x}_2) \qquad (47)$$

According to "Eq. (31)", the unknown coefficients for critical mode shape are calculated as follows ($r = 2, c_6 = 1, L_1 = L/4, L_2 = 3L/4$):

$$\begin{Bmatrix} c_1 \\ c_2 \\ c_3 \\ c_4 \\ c_5 \end{Bmatrix} = \begin{Bmatrix} 1.0827056/L \\ 1.109193504 \\ 0.270676391 \\ 1.0827056/L \\ 0.479906478 \end{Bmatrix} \qquad (48)$$

The unknown coefficients for second mode shape are:

$$\begin{Bmatrix} c_1 \\ c_2 \\ c_3 \\ c_4 \\ c_5 \end{Bmatrix} = \begin{Bmatrix} -1.059859/L \\ 1.068701814 \\ -0.26496478 \\ -1.059859/L \\ -0.37699279 \end{Bmatrix} \qquad (49)$$

The unknown coefficients for third mode shape are:

$$\begin{Bmatrix} c_1 \\ c_2 \\ c_3 \\ c_4 \\ c_5 \end{Bmatrix} = \begin{Bmatrix} 2.466708/L \\ 2.47706007 \\ 0.61667719 \\ 2.466708/L \\ -2.2662362 \end{Bmatrix} \qquad (50)$$

The first normalized mode shapes are illustrated in "Fig. 3".

6   RESULTS AND DISCUSSION

The diagram of characteristic equation of beam buckling for fractional material gradation in axial direction with pinned-clamped boundary conditions is depicted in "Fig. 4".
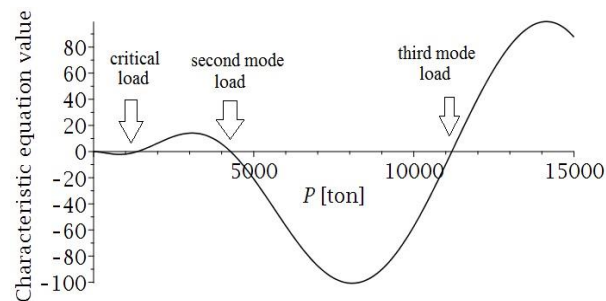
Fig. 4   Characteristic equation diagram for pinned-clamped ends.

The pinned and clamped supports are modeled by approaching $k_{\theta l}$ and $E_0 I/(L k_{\theta r})$ to zero. The mechanical and geometrical properties are $E_0 = 2 \times 10^6 \ kg/cm^2$, $L_1 = 20 cm$ and $L_2 = 40 cm$. The beam section is a square with 5cm side.

The intersection points of diagram with the horizontal axis (characteristic equation roots) are buckling loads of first modes. The first three buckling loads are 1362.81 ton, 4278.58 ton and 11186.58 ton. The normalized mode shapes are illustrated in "Fig. 5 to Fig. 7".
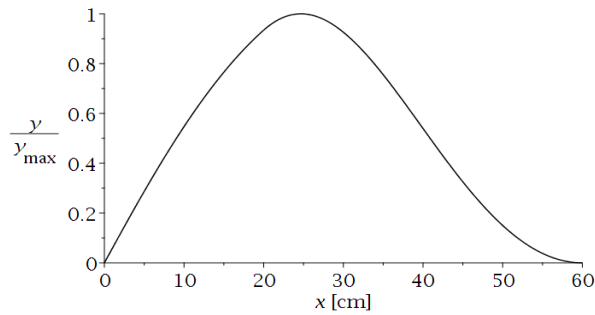
Fig. 5   Normalized first mode shape of axially graded beam.
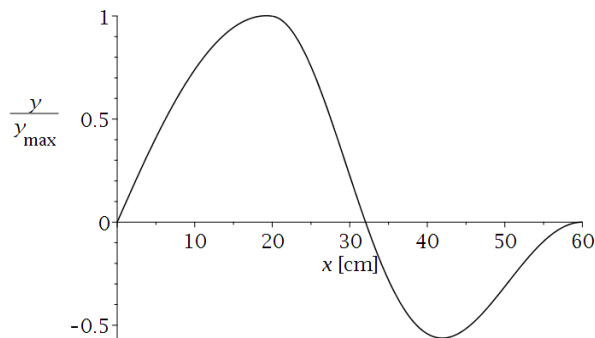
Fig. 6   Normalized second mode shape of axially graded beam.
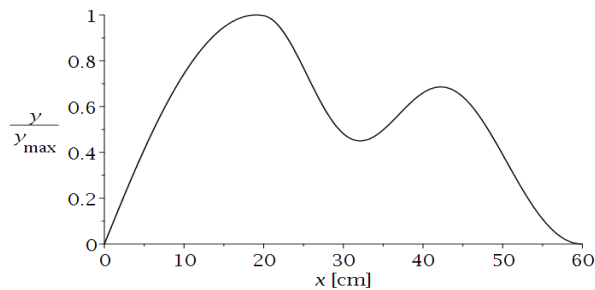
Fig. 7   Normalized third mode shape of axially graded beam.

The effects of rotational spring stiffness at semi-rigid supports on critical load of fractional axially graded beam subjected to axial span-load are presented in "Fig. 8". By increasing rotational stiffness, the critical load increases. The increase rate of critical load decreases by increasing rotational stiffness at semi-rigid restraints.
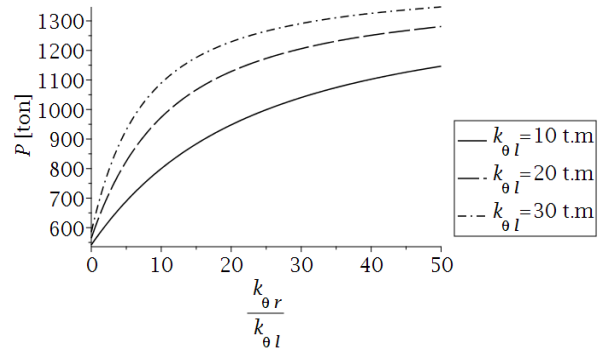
Fig. 6   The effect of rotational stiffness on critical load.

The effect of rotational stiffness on end rotations in first mode shape of stepwise fractional axially graded beam subjected to axial compression with piecewise load function is presented in "Fig. 9". The rotation of the beam ends decreases by increasing rotational stiffness. For mechanical and geometrical properties of beam assumed in this section, the maximum deflection is shifted to the left slightly by increasing rotational stiffness ($k_{\theta l} = k_{\theta r} = k_\theta$).
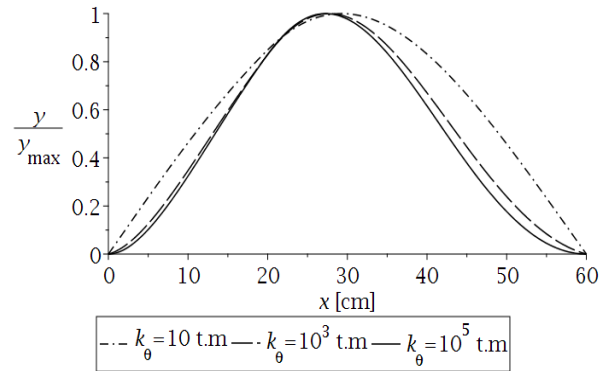
Fig. 9   The effect of rotational stiffness on mode shape.
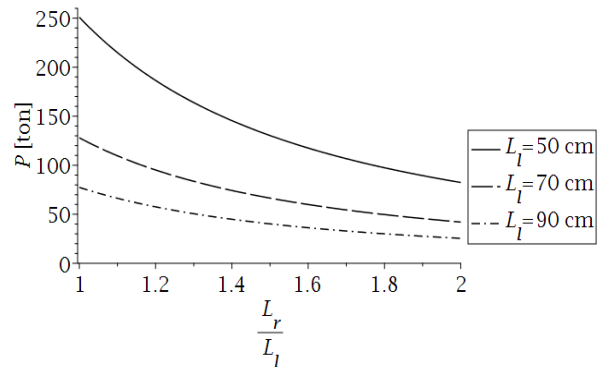
Fig. 10   The effect of two part lengths on critical load.

The critical load reduction of simply supported ($k_{\theta l} = k_{\theta r} = 0$) stepwise fractional axially graded beam subjected to axial span-load caused by increasing of two part lengths is illustrated in "Fig. 10".

7 CONCLUSION

For the first time, the buckling analysis of Euler-Bernoulli beam by considering discontinues material gradation in the axial direction with fractional pattern subjected to axial compressive load with piecewise function rested on semi-rigid restraints is conducted. In the limit state, the various boundary conditions including simply supported and clamped ends are modeled and numerical solutions are presented. The equilibrium differential equations of beam with and without axial compression are calculated by using variational calculus. The natural equations, deflection continuity as well as boundary conditions are written in the matrix form. The beam discretizing and nontrivial solution are employed to derive characteristic equation from reduced coefficient matrix by satisfying continuity, natural and boundary conditions. The corresponding mode shapes of first buckling loads are calculated by employing matrix operations. It is observed that the buckling load is decreased by increasing lengths of beam parts and increased by increasing rotational stiffness at semi-rigid supports. In the case of homogeneous beam, the result validity is proved by observing a good agreement between results of current work and well-known data in literature.

REFERENCES

[1]   She, G. L., Jiang, X. Y., and Karami, B., On Thermal Snap-Buckling of FG Curved Nano Beams, Materials Research Express, Vol. 6, No. 11, 2019, pp. 115008, https://doi.org/10.1088/2053-1591/ab44f1.

[2]   She, G. L., Ren Y., R., and Yuan, F. G., Hygro-Thermal Wave Propagation in Functionally Graded Double-Layered Nanotubes Systems, Steel and Composite Structures, Vol. 31, No. 6, 2019, pp. 641-653, https://doi.org/10.12989/scs.2019.31.6.641.

[3]   She, G. L., Ren Y., R., and Yan, K. M., On Snap-Buckling of Porous FG Curved Nano Beams, Acta Astronautica, Vol. 161, 2019, pp. 475-484, https://doi.org/10.1016/j.actaastro.2019.04.010.

[4]   She, G.L., Yuan, F. G., Karimi, B., Ren, Y. R., and Xiao, W. S., On Nonlinear Bending Behaviour of FG Porous Curved Nanotubes, International Journal of Engineering Science, Vol. 135, 2019, pp. 58-74, https://doi.org/10.1016/j.ijengsci.2018.11.005.

[5]   She G. L., Yan K. M., Zhang Y. L., Liu H. B., and Ren Y. R., Wave Propagation of Functionally Graded Porous Nano Beams Based On Non-Local Strain Gradient Theory, The European Physical Journal Plus, Vol. 133, 2018, pp. 58-74, https://doi.org/10.1140/epjp/i2018-12196-5.

[6]   She, G. L., Yuan, F. G., Ren, Y. R., Liu, H. B., and Xiao, W. S., Nonlinear Bending and Vibration Analysis of Functionally Graded Porous Tubes Via a Nonlocal Strain Gradient Theory, Composite Structures, Vol. 203, 2018, pp. 614-623, https://doi.org/10.1016/j.compstruct.2018.07.063.

[7]   She, G. L., Yuan F. G., and Ren, Y. R., On Wave Propagation of Porous Nanotubes, International Journal of Engineering Science, Vol. 130, 2018, pp. 62-74, https://doi.org/10.1016/j.ijengsci.2018.05.002.

[8]   She, G. L., Ren, Y. R., Yuan F. G., and Xiao, W. S., On Vibrations of Porous Nanotubes, International Journal of Engineering Science, Vol. 125, 2018, pp. 23-35, https://doi.org/10.1016/j.ijengsci.2017.12.009.

[9]   She, G. L., Yuan F. G., Ren, Y. R., and Xiao, W. S., On Buckling and Postbuckling Behaviour of Nanotubes, International Journal of Engineering Science, Vol. 121, 2017, pp. 130-142, https://doi.org/10.1016/j.ijengsci.2017.09.005.

[10] She, G. L., Yuan F. G., and Ren, Y. R., Thermal Buckling and Post-Buckling Analysis of Functionally Graded Beams Based On a General Higher-Order Shear Deformation Theory, Applied Mathematical Modelling, Vol. 47, 2017, pp. 340-357, https://doi.org/10.1016/j.apm.2017.03.014.

[11] Toghroli, A., Darvishmoghaddam, E., Zandi, Y., Parvan, M., Safa, M., Abdullahi, M. M., Heydari, A., Wakil, K., Gebreel, S. A. M., and Khorami, M., Evaluation of the Parameters Affecting the Schmidt Rebound Hammer Reading Using ANFIS Method, Computers and Concrete, Vol. 21, No. 5, 2018, pp. 525-530, https://doi.org/10.12989/cac.2018.21.5.525.

[12] Heydari, A., Elasto-Plastic Analysis of Cylindrical Vessel with Arbitrary Material Gradation Subjected to Thermo-Mechanical Loading via DTM, Arabian Journal for Science and Engineering, Vol. 44, No. 10, 2019, pp. 8875–8891, https://doi.org/10.1007/s13369-019-03910-x.

[13] Ismail, M., Shariati, M., Awal, A., Chiong, C., Chahnasir, E., Porbar, A., Heydari, A., and Khorami, M., Strengthening of Bolted Shear Joints in Industrialized Ferrocement Construction, Steel and Composite Structures, Vol. 28, No. 6, 2018, pp. 681-690, DOI: https://doi.org/10.12989/scs.2018.28.6.681.

[14] Heydari, A., Spreading of Plastic Zones in Functionally Graded Spherical Tanks Subjected to Internal Pressure and Temperature Gradient Combinations, Iranian Journal of Mechanical Engineering Transactions of the ISME, Vol. 16, No. 2, 2015, pp. 5-25.

[15] Heydari, A., Shariati, M., Buckling Analysis of Tapered Bdfgm Nano-Beam Under Variable Axial Compression Resting On Elastic Medium, Structural Engineering and Mechanics, Vol. 66, No. 6, 2018, pp. 737-748, https://doi.org/10.12989/sem.2018.66.6.737.

[16] Heydari, A., Jalali, A., and Nemati, A., Buckling Analysis of Circular Functionally Graded Plate Under Uniform Radial Compression Including Shear Deformation with Linear and Quadratic Thickness Variation On the Pasternak Elastic Foundation, Applied Mathematical Modelling, Vol. 41, 2017, pp. 494-507, https://doi.org/10.1016/j.apm.2016.09.012.

[17] Heydari, A., Size-Dependent Damped Vibration and Buckling Analyses of Bidirectional Functionally Graded Solid Circular Nano-Plate with Arbitrary Thickness Variation, Structural Engineering and Mechanics, Vol. 68, No. 2, 2018, pp. 171-182, https://doi.org/10.12989/sem.2018.68.2.171.

[18] Heydari, A., Exact Vibration and Buckling Analyses of Arbitrary Gradation of Nano-Higher Order Rectangular Beam, Steel and Composite Structures, Vol. 28, No. 5, 2018, pp. 589-606, https://doi.org/10.12989/scs.2018.28.5.589.

[19] Heydari, A., Exact Vibration and Buckling Analyses of Arbitrary Gradation of Nano-Higher Order Rectangular Beam, Steel and Composite Structures, Vol. 28, No. 5, 2018, pp. 589-606, https://doi.org/10.12989/scs.2018.28.5.589.

[20] Heydari, A., Buckling of Functionally Graded Beams with Rectangular and Annular Sections Subjected to Axial Compression, Journal of Advanced Design and Manufacturing Technology, Vol. 5, No. 1, 2011, pp. 25-31.

[21] Heydari, A., Analytical Solutions for Buckling of Functionally Graded Circular Plates Under Uniform Radial Compression Using Bessel Function, Journal of Advanced Design and Manufacturing Technology, Vol. 6, No. 4, 2013, pp. 41-47.

[22] Heydari, A., Elasto-Plastic Analysis of Thick Walled FG Tanks Subjected to The Internal Pressure, Journal of Advanced Design and Manufacturing Technology, Vol. 3, No. 1, 2009, pp. 11-18.

[23] Heydari, A., Sheykhepour, M., Critical Load of Beam with Linear and Quadratic Axial Gradation Rested On Rotational Spring Hinge, The Second International Conference On Innovation and Research in Engineering, Tbilisi, Georgia, 2019.

[24] Heydari, A., Ghanizade, M., The Effect of Attached Lumped Mass Position On the Frequency Reduction of the Radially Graded Tube, 6th National Conference On Applied Research in Civil Engineering, Architecture and Urban Management, Tehran, Iran, 2019.

[25] Heydari, A., Elastic Buckling Analysis of Multistory Functionally Graded Sway Bending Frame Via Finite Element Method, The Second International Conference On Innovation and Research in Engineering, Tbilisi, Georgia, 2019.

[26] Heydari, A., Buckling Analysis of Multistory Axisymmetric Functionally Graded Bending Frames with Semi-Rigid Connections, 7th International Conference On Civil Engineering, Architecture and Urban Economy Development, Shiraz, Iran, 2018.